# Determining the Susceptibility of Cloud Albedo to Changes in Droplet Concentration with the Advanced Very High Resolution Radiometer

S. PLATNICK

*Institute of Atmospheric Physics, University of Arizona, Tucson, Arizona*

S. TWOMEY

(Manuscript received 22 January 1993, in final form 6 October 1993)

ABSTRACT

Combustion processes that produce greenhouse gases also increase cloud condensation nuclei (CCN) concentrations, which in turn increase cloud droplet concentrations and thereby cloud albedo. A calculation of *cloud susceptibility*, defined in this work as the increase in albedo resulting from the addition of one cloud droplet per cubic centimeter (as cloud liquid water content remains constant), is made through the satellite remote sensing of cloud droplet radius and optical thickness. The remote technique uses spectral channels of the Advanced Very High Resolution Radiometer (AVHRR) instrument on board NOAA polar-orbiting satellites. Radiative transfer calculations of reflectance and effective surface and cloud emissivities are made for applicable sun and satellite viewing angles, including azimuth, at various radii and optical thicknesses for each AVHRR channel. Emission in channel 3 (at 3.75 $\mu$m) is removed to give the reflected solar component. These calculations are used to infer the radius and optical thickness that best match the satellite measurements. An approximation for the effect of the atmosphere on the signal received by the AVHRR is included in the analysis. Marine stratus clouds, as well as being important modifiers of climate, are cleaner than continental clouds and so likely to be of higher susceptibility. Analysis of several stratus scenes, including some containing ship tracks, supports this expectation. The retrieved range of susceptibilities for all marine stratus clouds studied varied by about two orders of magnitude. This variation implies that climate studies that include possible marine stratus albedo modification from anthropogenic CCN are incomplete without accounting for existing susceptibilities.

## 1. Introduction

With much attention being given to $CO_2$ and other greenhouse gases, it is important to appreciate that water is the most critical radiative species in the atmosphere, both as a vapor and as liquid or ice in clouds. Clouds have been recognized as the most significant modulators to radiative processes in the atmosphere. Calculations for the overall radiative effect of clouds compared with a clear-sky earth, based on satellite observations reported by various researchers, indicate that on a global scale clouds have a cooling influence, though the magnitude of this so-called *cloud forcing* varies by a factor of 2 between the studies [see Arking (1991) for review]. Knowing the present influence of clouds does not, however, indicate the climatic response to a modification in a particular cloud parameter.

It is the *cloud sensitivity* (Arking 1991), defined as the change in energy absorbed by the climate system to changes in a cloud parameter, that is meaningful for climate change. Important cloud parameters include the macroscopic (such as cloud amount, or cloud cover fraction, and cloud height and thickness) and the microscopic (cloud liquid water content, droplet size, and phase). An important cloud microphysical parameter, not typically incorporated into GCMs, is droplet size. Cloud reflectance is partially dependent on droplet size, which is in turn linked with cloud condensation nuclei (CCN) concentrations present during cloud development (Twomey 1974). CCN concentrations are variable, having both natural and anthropogenic sources. Among the anthropogenic sources are combustion processes that also release $CO_2$, a major greenhouse gas. The overall effect of increasing CCN is to increase cloud albedo, which results in cooling; there is no compensating effect in the infrared. This so-called indirect effect of aerosols on the radiation budget has been estimated to be comparable to greenhouse forcing but opposite in sign (Charlson et al. 1992). In light of these concerns, it is useful to define a quantity representing the *sensitivity* of cloud albedo to changes in CCN concentration. This quantity is referred to as *cloud susceptibility*. It is reasonable to believe that the macroscopic cloud parameters such as cloud amount and some of the microscopic parameters (such as liquid

*Corresponding author address:* Dr. Steven Platnick, NASA Goddard Space Flight Center, Code 913, Greenbelt, MD 20771.

water content) might be substantially altered only through large-scale changes in climate and that direct anthropogenic modification could be expected only on a local scale, if even there. For such parameters, an initial change in climate is necessary to begin a cloud–climate feedback process. However, this is not true of droplet size, which can be directly altered. The modification of cloud albedo by CCN does not solely constitute a feedback and can develop independent of any actual climate change. It is referred to as a *climate forcing* mechanism.

As expected, not all clouds are equally susceptible; the determining factors are primarily cloud optical thickness and droplet size. Both can be inferred remotely through solar reflection measurements at wavelengths that are absorbing and nonabsorbing for liquid water. Since global susceptibility is of importance for climate, a satellite remote sensing scheme has been developed using the Advanced Very High Resolution Radiometer (AVHRR) aboard the National Oceanic and Atmospheric Administration (NOAA) polar-orbiting satellites. Channel 3 of the AVHRR, at 3.75 $\mu$m, provides the absorbing wavelength. Thermal emission by the cloud and surface at this wavelength contaminates the solar reflected signal. Brightness temperature in channel 4, in the thermal infrared, is used to estimate this emission. This study primarily investigates maritime stratus clouds, which are expected to be cleaner and so have the greatest susceptibilities to albedo modification. Results for a number of these stratus scenes are presented.

## 2. Susceptibility

The ultimate fate for a given wavelength of the incident radiation is partially dependent on the cloud drop density $N$, which may range from 10 cm$^{-3}$ for very clean air to thousands per cubic centimeter for continental or polluted air. The final droplet density is approximately proportional to the number density of CCN present during cloud formation (Twomey 1959). Experimental data of CCN versus supersaturation (Twomey and Wojciechowski 1969) and measurements of both CCN and $N$ by Twomey and Warner (1967) gave an approximate linear fit between CCN and droplet concentration. Recent studies by Hudson and Rogers (1986) and Hegg et al. (1991) showed similar results.

Most CCN are thought to be sulfates (Twomey 1968; Dinger et al. 1970). Natural sources of sulfur include volcanic and biological activity. Over the oceans dimethyl sulfide (DMS) excreted by phytoplankton is believed a significant contributor (Charlson et al. 1987). For critical supersaturations below 1%, the difference in CCN concentrations between continental and clean maritime air can easily be greater than an order of magnitude (Twomey and Wojciechowski 1969). Combustion processes are also found to be an abundant source for CCN (e.g., Squires 1966; Warner and Twomey 1967; Gorbinet and Serpoly 1985). Hobbs et al. (1980) made measurements of elevated CCN in power plant plumes and found order of magnitude increases of cloud droplet numbers in clean marine stratus affected by the plume. Leaitch et al. (1992) examined continental clouds and found a correlation between cloud droplet concentrations and pollution as determined by cloud water sulfate concentrations.

Twomey (1974) proposed a link between pollution and cloud albedo. Since combustion processes are known to be prolific sources of CCN, a cloud forming in a polluted air mass will end up with a larger concentration of cloud droplets than for the same cloud developing under identical circumstances in cleaner air. For a homogeneous cloud layer with geometrical thickness $\Delta h$, the optical thickness is

$$\tau = \int Q_e(r/\lambda)\pi r^2 n(r)\,dr\Delta h$$

$$= \frac{\pi \int Q_e(r/\lambda) r^2 n(r)\,dr}{\int r^2 n(r)\,dr} \frac{\int r^2 n(r)\,dr}{\int n(r)\,dr} \int n(r)\,dr\Delta h$$

$$= \overline{Q_e}\pi\overline{r^2} N\Delta h = \overline{Q_e}\pi r_{\rm rms}^2 N\Delta h, \qquad (1)$$

where $n(r)$ is the droplet size distribution, $r_{\rm rms}$ the root-mean-square radius of the size distribution, and $\overline{Q_e}$ is the average extinction efficiency, which has reached its asymptotic value ($\approx 2$) in the visible and much of the near infrared for the range of droplet sizes expected. So as droplet concentrations increase, all else remaining constant, optical thickness increases ($\tau \propto r_{\rm rms}^2 N$), which in turn leads to an increase in cloud albedo. But it is reasonable to assume that clouds forming under the same set of circumstances, but with different CCN amounts, will have the same supply of vapor available for droplet growth. For such a case the liquid water content $W$ of the mature clouds can be expected to be equivalent, so that droplet sizes in the polluted cloud would be smaller than those for the clean cloud. Therefore, under the condition of constant liquid water content, there is the competing effect on optical thickness of larger droplet concentration versus smaller droplet size. Liquid water content can be expressed as

$$W = \rho_w \frac{4}{3}\pi \int r^3 n(r)\,dr$$

$$= \rho_w \frac{4}{3}\pi \frac{\int r^3 n(r)\,dr}{\int n(r)\,dr} \int n(r)\,dr$$

$$= \rho_w \frac{4}{3}\pi \overline{r^3} N = \rho_w \frac{4}{3}\pi r_v^3 N, \qquad (2)$$

where $r_v$ is a volume-weighted moment of the size distribution and $\rho_w$ is the density of liquid water. A third measure of the size distribution, used in the radiative transfer calculations that follow, is the effective radius (Hansen and Travis 1974), defined as

$$r_{\text{eff}} = \frac{\int r^3 n(r) dr}{\int r^2 n(r) dr} = \frac{r_v^3}{r_{\text{rms}}^2}. \tag{3}$$

It is the effective radius that is retrieved from cloud reflection measurements. For the relatively narrow size distributions found in marine stratus there is typically little difference between $r_{\text{eff}}$, $r_v$, and $r_{\text{rms}}$, and these radii can be interchanged in the manipulation of the above equations. Such a conclusion was reached by Grassl (1982) based on analysis of measured and assumed size distributions. As an example, Martin and Johnson (1992) analyzed measurements of droplet size distributions and liquid water contents in stratocumulus off the southern coast of California and near the United Kingdom and proposed the linear regression $r_v = kr_{\text{eff}}$, where $k \approx 0.93$. With Eq. (3) this regression also implies that $r_v = k^{-1/2} r_{\text{rms}}$ (or $r_v \approx 1.04 r_{\text{rms}}$). Fouquart et al. (1990) also suggested this linear relation. An implicit assumption in such a regression is that $k$ is not a function of number concentration, at least for the clouds analyzed. Ignoring differences in $r_v$ and $r_{\text{rms}}$, Eqs. (1) and (2) give the following expression for optical thickness under the condition of constant liquid water content:

$$\tau = \overline{Q_e} \pi \left[ \frac{W}{\rho_w (4/3)\pi} \right]^{2/3} N^{1/3} \Delta h. \tag{4}$$

Consequently, $\tau \propto N^{1/3}$.

The question then arises as to the significance of the albedo change. Clouds formed in clean maritime air having low CCN concentrations are more susceptible than those formed in particle-rich continental air. When the albedo $A$, $N$, and $\Delta N$ are known, a calculation can be made for the change in albedo, but since $\Delta N$ is variable it is useful to define a parameter that will characterize the sensitivity of albedo to changes in droplet concentration. The derivative $dA/dN$ (approximately equivalent to choosing $\Delta N = 1$) represents such a link (Twomey 1989). Since, in general, $A = A(\tau, \bar{\omega}_0, g)$, the derivative can be expressed in the form

$$\frac{dA}{dN} = \frac{\partial A}{\partial \tau}\frac{d\tau}{dN} + \frac{\partial A}{\partial \bar{\omega}_0}\frac{d\bar{\omega}_0}{dN} + \frac{\partial A}{\partial g}\frac{dg}{dN} \tag{5}$$

and under the condition of constant liquid water content will be termed *cloud susceptibility.* Note that all terms are wavelength dependent. For the special case of conservative scattering, which in the absence of significant aerosol absorption is applicable in the visible where about one-half of solar flux occurs, $\bar{\omega}_0 = 1$ and $g$ is approximately constant with radius, so the last two terms in Eq. (5) can be neglected. With Eq. (4), susceptibility reduces to

$$\frac{dA}{dN} = \frac{\partial A}{\partial \tau}\frac{\tau}{3N} = \frac{4\pi\rho_w}{9W}\tau\frac{\partial A}{\partial \tau} r_v^3, \tag{6}$$

where either $N$, or $r_v$ and $W$ can be used as an independent variable. Of obvious note is the strong radius dependence in the second form. Cloud susceptibility is primarily a function of droplet radius and optical thickness. The global effect of increasing CCN concentration depends on geographical and temporal distributions of these two parameters (for clouds with significant transmission, global susceptibility also depends on the distribution of the reflectance of the underlying surface).

Equation (6) has been derived ignoring differences in $r_v$ and $r_{\text{rms}}$ (Grassl 1982). It can be shown that the equation holds exactly when assuming the linear relation $r_v = kr_{\text{eff}}$ (or $r_v = k^{-1/2} r_{\text{rms}}$) like that of Martin and Johnson (1992) and Fouquart et al. (1990) as discussed previously, even though Eq. (4) must be multiplied by the additional factor $k$. With such an assumption, $r_v^3$ in Eq. (6) may be replaced by $(kr_{\text{eff}})^3$ if $k$ is known ($k^3 \approx 0.81$ using the results of Martin and Johnson). For present purposes, however, no further distinction between the moments will be made and all subsequent references to radius in Eq. (6) will be understood to mean the radius that is inferred from the satellite reflection measurements, that is, the effective radius.

Though numerical calculations are generally needed for determining $\partial A/\partial \tau$, the two-stream analytic approximation (Bohren 1980) provides some simple insight. For conservative scattering, the two-stream approximation gives $A \approx [(1-g)\tau][2 + (1-g)\tau]^{-1}$. The term $\tau \partial A/\partial \tau$ in Eq. (6) is then given as $A(1-A)$, regardless of $g$, which has a maximum at an albedo of 0.5 or an optical thickness of about 13. When multiplied by $r^3$ (and the term containing liquid water content) this expression becomes susceptibility. Calculations with a detailed radiative transfer code also give a peak in susceptibility at 50% albedo for all radii. The two-stream approximation can also be used to show albedo changes due to nondifferential changes in droplet concentration. Consider a cloud having droplet concentration $N$. If $N$ is changed by some factor $\chi$ (i.e., $N \rightarrow \chi N$), then $\tau \rightarrow \chi^{1/3}\tau$ and

$$\Delta A = [A(1-A)(\chi^{1/3} - 1)][A(\chi^{1/3} - 1) + 1]^{-1}. \tag{7}$$

For example, at $A = 0.5$, a doubling in $N$ will increase albedo to a value of about 0.56. It can be shown from Eq. (7) that, similar to susceptibility, the peak in $\Delta A$ occurs very close to $A = 0.5$ for reasonable $\chi$ ($<2$).

The notable point in the previous development is that existing cloud microphysics is essential in deter-

mining the climate forcing by CCN. Cloud climatologies give cloud albedo, which may be adequate for understanding the current shortwave energy balance but is not sufficient for estimating changes in the energy balance; cloud microphysics must also be known. Estimates of the cloud forcing due to increasing CCN typically assumes that droplet concentrations in clean maritime clouds increase by some factor (e.g., Charlson et al. 1992; Penner et al. 1992; Kaufman et al. 1992; Ghan et al. 1990). While changes in other climate modifiers, such as $CO_2$, may be usefully expressed in this way, the same is not true of droplet concentration. For example, pollution is more likely to increase CCN concentrations by some absolute number, say a few per cubic centimeter, over some geographical region. The effect on a cloud that would otherwise have droplet concentrations of 10 $cm^{-3}$ can be very different than for a cloud having the same albedo but with $N = 100$ $cm^{-3}$ (and a smaller geometrical thickness). Each will respond differently to the increase in droplet concentration [see Eq. (7)]. It is not at all clear that every maritime cloud should have about the same droplet concentration, which is one of the underlying assumptions of using a factor increase in $N$ to model albedo modification. In addition to albedo, droplet concentration must be known, and simple assumptions about the microphysics can be misleading. Any figure of merit for susceptibility must have a two-dimensional functional dependence that will include albedo (or optical thickness) and a microphysical variable (e.g., $A$ and $N$, $A$ and $r$, $\tau$ and $r$, $A$ and $\chi$); the exact definition is largely irrelevant.

The previous analysis was for conservative scattering, applicable in the visible. Susceptibility of the broadband albedo would involve a calculation where all terms in Eq. (5) would have to be addressed. An easier, though approximate, approach is to find a relation for broadband albedo based on the albedo for a visible wavelength and apply this to susceptibility. Several studies have attempted to find a regression between narrowband albedo in the visible and the integrated broadband calculation. The spectral albedo of clouds decreases into the near infrared due to increasing absorption by liquid water, so it is expected that visible albedo exceeds the broadband. The difference will depend on cloud optical thickness and microphysics. Numerical studies by Wydick et al. (1987) using channel 1 of the AVHRR (used in this study) gave the linear approximation $\langle A \rangle_\lambda = 0.8A_{\text{vis}} + 0.0078$ as a fit for all cloud optical thicknesses considered. Apart from the small offset, $A_{\text{vis}}$ overestimated broadband albedo by 25%. Shine et al. (1984) made a similar study for the AVHRR channel 1. For clouds with optical thicknesses of 10–30, broadband albedo was overestimated by 12%–20%, respectively, using a midlatitude model. Results from Laszlo et al. (1988) are similar. If a linear regression is appropriate, then the integrated susceptibility can be approximated by

$$\frac{d\langle A \rangle_\lambda}{dN} = \alpha \frac{dA_{\text{vis}}}{dN}, \tag{8}$$

with $\alpha$ being the slope of the fit ($\approx$0.8–0.9). Further mention of susceptibility will imply the narrowband visible value.

Though marine stratus are notorious for their longevity, Albrecht (1989) has reported measuring drizzle drops (>40-$\mu$m radii) in these clouds and concluded that precipitation must be occurring. He theorizes that increases in CCN in clean maritime clouds, which decrease the mean drop size, will decrease the production of drizzle drops. Consequently the clouds would contain a higher liquid water content. Such a connection, if generally true of marine stratus, would suggest that defining susceptibility for a process of constant liquid water content should be modified to allow for an increase. This would serve to further enhance cloud brightening. Measurements by Radke et al. (1989) showed increased liquid water content inside ship tracks compared with cloud areas away from the tracks. The applicability of ship tracks to the general case of marine stratus modification by global increases in CCN is not certain. It is likely that the development of the track, with respect to surrounding stratus, can be affected by the ship's passage in ways other than CCN production alone. In contrast, a more general study was made on continental clouds by Leaitch et al. (1992). Their multiseason and multiyear measurements made over Ontario and New York State showed a positive correlation between cloud droplet concentrations and anthropogenic pollution (as measured by cloud water sulfate concentrations) but showed that cloud liquid water content was invariant to pollution amounts. Nevertheless, it is useful to consider the consequences of relaxing the constant liquid water content assumption.

Suppose some type of power law to relate liquid water content to droplet concentration of the form $W = \alpha N^\beta$. With $0 < \beta < 1$ the liquid water content of the mature cloud asymptotically approaches a limiting value as $N$ increases; that is, it becomes increasingly more difficult to have drizzle with large $N$. This is about the only characteristic such a relation must have based on the hypothesis. Measurements in and out of ship tracks taken by Radke et al. give $W \approx 0.3$ g $m^{-3}$ and 0.5 g $m^{-3}$ for $N \approx 30$ $cm^{-3}$ and 100 $cm^{-3}$, respectively (implying $\alpha \approx 0.07$ g $m^{-3}$ and $\beta \approx 0.42$). Then

$$r^2 = \left(\frac{3\alpha}{4\pi\rho_w} N^{\beta-1}\right)^{2/3},$$

which can be used in the definition of optical thickness. Then the derivative $d\tau/dN$ gives a susceptibility of

$$\frac{\partial A}{\partial \tau}\frac{\tau}{3N}(1 + 2\beta) = \left(\frac{4\pi\rho_w}{9W}\right)\tau \frac{\partial A}{\partial \tau} r^3(1 + 2\beta). \tag{9}$$

The result is identical to Eq. (6) with the exception of the factor $1 + 2\beta$; for constant liquid water content, $\beta = 0$ and the two equations are identical. With the measurements of Radke et al. the factor becomes about 1.8 indicating that susceptibility would be increased by 80% over the constant liquid water content assumption for all initial values of $W$. As with Eq. (6), knowledge of the initial liquid water content is still needed for the expression containing radius. In light of the critical dependencies of susceptibility on radius (or $N$) and optical thickness, this underestimation of about 40% seems minor. Uncertainty involving the need to even account for changing liquid water content suggests that the original definition of susceptibility is both adequate and preferable.

The process defined by susceptibility is the dominant radiation influence of particulate pollution (at least for reasonably clean clouds with typical albedos). Grassl (1982) found little effect in the infrared. Pollution is also a source of carboniferous aerosol, which absorbs in the visible. This effect on cloud albedo, considered by Twomey (1977) and Grassl, can be seen only in the brightest clouds.

## 3. The remote sensing of susceptibility

The method of inferring droplet radius through near-infrared absorption has been used by a number of investigators (e.g., Twomey and Cocks 1982, 1989; Stephens and Platt 1987; Foot 1988; Rawlins and Foot 1990) using aircraft-borne sensors. Two or more near-infrared wavelengths were used though none of these aircraft investigations made measurements in the 3.75-$\mu$m window. In situ cloud measurements typically showed that droplet radius was overestimated by 2–5 $\mu$m. Retrieving larger droplets implies that the observed $\bar{\omega}_0$ is lower than would be expected from calculations based on measured droplet sizes. This has been termed anomalous absorption. Stephens and Tsay (1990) give a review of the measurements and comment on proposed causes of the anomaly. Suggested causes include continuum vapor absorption in the windows and cloud inhomogeneities. Taylor (1992) has reported that improvements in the band models used for atmospheric absorbers in LOWTRAN 7 explained the anomalously high retrieved radii of Rawlins and Foot (1990), who corrected for atmospheric effects with the earlier version LOWTRAN 5. It is not clear whether radius inferred from a 3.75-$\mu$m channel would suffer from such an anomaly. With a much larger liquid water absorption (order of magnitude greater than at 2.2 $\mu$m), the mean number of scatterings for reflected photons would be less (about 8 at $\tau = 10$ versus 20 for conservative scattering) and photon penetration into the cloud, both vertically and horizontally, would be reduced, implying that the effect of inhomogeneities would be less. The large liquid water absorption might also tend to mask out any unaccounted-for continuum vapor absorption.

Arking and Childs (1985) used the AVHRR for remote sensing of cloud droplet radii and optical thickness although no in situ cloud measurements were used for validation. Grainger (1990) used the AVHRR for studying orographic effects on droplet sizes. Emission at 3.75 $\mu$m is comparable to, and can even exceed, the reflected radiation. Figure 1a shows bidirectional reflectance in AVHRR channel 3. Figure 1b shows the ratio of reflected solar radiation to emission; the two are seen to be equal for droplet radii of about 10 $\mu$m. Optical thickness has been scaled by $2/Q_{ext}$ in the figures and all other results that follow. This gives an optical thickness appropriate at visible wavelengths and provides a common abscissa for all radii and all channels. While removing emission is certainly an added

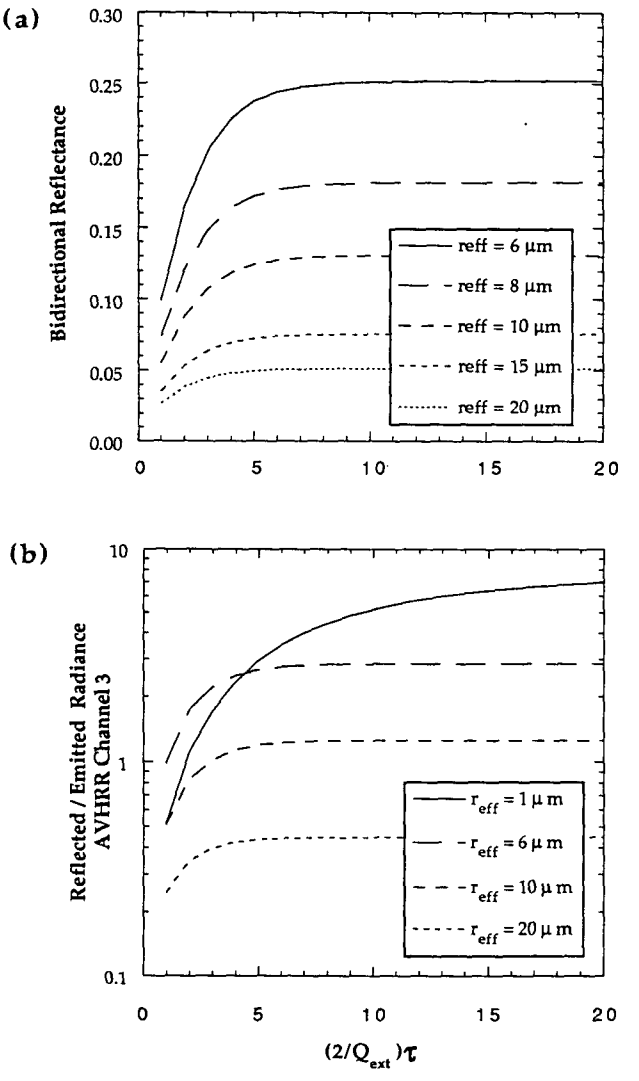


FIG. 1. Calculations for AVHRR channel 3 (3.75 $\mu$m) of (a) bidirectional reflectance and (b) the ratio of reflected solar radiance to thermal emission. Calculated with $\mu_0 = 0.75$, $\mu_{sat} = 0.85$, and using the azimuthal average for reflection. Channel 3 calculations made with surface and cloud temperatures of 290 K.

complication, the large absorption in the channel does give its use one very important advantage—the signal is almost entirely dependent on radius, with very little optical thickness sensitivity except for the thinnest clouds. Shorter wavelengths have substantial optical thickness dependencies over much of the expected radius range. The substantial radius information content of a 3.75-$\mu$m channel makes it of special interest for remote sensing regardless of its status as a major contender for satellite studies.

The determination of bidirectional solar reflectance and emission seen by the satellite, given cloud optical thickness and radius, represents the *forward* problem and is calculated using the doubling or adding matrix method of Twomey et al. (1966). Inferring optical thickness and droplet radius from satellite reflection and emission data characterizes an *inverse* problem that, in this study, is decided by the best fit between the satellite measurement and various entries in a library file. The library contains bidirectional reflectances for AVHRR channels 1, 2, and 3 (center wavelengths at 0.65, 0.85, and 3.75 $\mu$m, respectively). Effective cloud and surface emissivities are calculated for channels 3, 4, and 5 (the latter two channels at about 10.75 and 12.0 $\mu$m, respectively). Use of an effective cloud emissivity assumes that the cloud is isothermal such that emitted cloud radiance is equal to the product of the effective emissivity and the Planck function at cloud temperature. The effective surface emissivity is used in a similar way to account for surface emission transmitted through the cloud. Cloud temperature is estimated by applying an atmospheric correction to the channel 4 brightness temperature. Sea surface temperature is determined from a split-window technique using channels 4 and 5 (McClain et al. 1985). The contents of the library include calculations for all combinations of the following: radii equal to 1, 4, 6, 8, 10, 12.5, 15, 17.5, 20, 25, 30, 35, and 45 $\mu$m; $\tau$ = 1, 2, $\cdots$, 60, 70, $\cdots$, 150; harmonics up to 20th order for the azimuthally dependent bidirectional reflectance (typically 5–10 harmonics are sufficient). Radii are the mean of a normal distribution with a dispersion of 0.2 (implying that $r_{\text{eff}} \approx 1.08 r_{\text{mean}}$). Radii increments were chosen based on uncertainty in likely retrieval errors (e.g., uncertainty in channel 3 emission and the atmospheric correction).

The effect of the atmosphere on the signal received by the satellite was modeled using the LOWTRAN 7 radiation code (Kneizys et al. 1988). The primary effects include the transmission of emitted radiation and direct and reflected solar radiation (important in all five AVHRR channels), solar radiation reflected from the atmosphere without ever encountering a cloud or surface (channels 1, 2, and 3), and direct emission from the atmosphere (channels 3, 4, and 5). Multiple reflections with the atmosphere are ignored. Calculations were made for two atmospheric paths: from the top of the atmosphere to sea level and to the top of the boundary layer (assumed to be cloud top). Midlatitude summer (MLS) and winter (MLW) standard atmospheres were analyzed; the Navy Maritime Aerosol Model was used with both. All effects depend on the satellite viewing angle and, for reflectance, solar angle as well. Given the uncertainties in having quantified these effects and the validity in using the model atmospheres, it was concluded that a single value of correction for each path and all viewing angles would be as far as the analysis should be carried. Satellite viewing angles are limited to 45° ($\mu$ = 0.7), if possible, to avoid the large variations associated with the increasing atmospheric optical depths. With this restriction, the rms satellite viewing angle turns out to be about 25° ($\mu$ = 0.9); a single atmospheric correction was chosen as the average of the MLS and MLW model atmospheres at this angle. An exception is made for extreme satellite viewing angles where a separate calculation is used. For reflectance, a solar angle of 25° was also used and an additional average of the 0° and 180° satellite solar azimuth angle was done. The effect of in-cloud vapor absorption on droplet single scattering albedo in the 3.75-$\mu$m channel was calculated from the HITRAN database using the $k$-distribution method (Arking and Grossman 1972) and found to be insignificant.

The surface, assumed to be the ocean for this study, is considered Lambertian to diffuse radiation with albedos of 0.06, 0.03, 0.01, 0.0, and 0.0 for channels 1–5, respectively. Clear-sky ocean radiances from an HRPT (high-resolution picture transmission) image, with satellite views away from the sun, showed consistency with the above-mentioned surface reflectances and the nominal atmospheric correction. Integration of the radiative properties over the finite band of each AVHRR channel is included in the calculations. Practically, only channels 1, 3, and 4 were needed. Channel 5 is used only with channel 4 in a split-window technique for inferring sea surface temperature.

Tests of the retrieval algorithm showed that the error function used to match measured radiances with library entries permitted multiple solutions when cloud droplet radii were 1 $\mu$m and optical thicknesses were less than the asymptotic limit for this radius. It appears that the small extinction efficiency for this radius in channel 3 is mainly responsible ($Q_{\text{ext}} \approx 0.75$ for a droplet radius of 1 $\mu$m versus 2.5 for a radius of 4 $\mu$m). Such a small droplet size is not expected for marine stratus, and so radii of 1 $\mu$m were eliminated from the possible solution set. No multiple solutions were found when restricting library radii to 4 $\mu$m and larger.

Channels 1 and 2 lack on-board calibration and must, without in-flight techniques, rely on calibrations typically performed several years before launch. In-flight calibrations with scenes of known reflectance show that the sensor response is modified from the preflight calibration (see Teillet et al. 1990). All *NOAA-11* channel 1 and 2 data in this study use the calibration coefficients of Che et al. (1991). The in-

flight calibration made closest in time to the recording of the data being studied is chosen. *NOAA-9* and *NOAA-10* AVHRR data is calibrated in the same way with the Teillet et al. gain values. These in-flight calibrations were made in terms of a reflected intensity. This is converted to albedo using the solar flux data of Neckel and Labs (1984).

Cloud liquid water content cannot be determined from solar reflection measurements alone. Though liquid water content is variable in marine stratus, it is quasi-constant when averaged over scales on the size of the AVHRR footprint and has a typical value of 0.3 g $m^{-3}$, which seems to be independent of locale (e.g., Feigelson 1978; Slingo et al. 1982; Noonkester 1984; Somerville and Remer 1984; Radke et al. 1989). In results that follow, susceptibility has been normalized to this value. All calculations of susceptibilities are made using the solar zenith angle at the time of the satellite overpass. Because of large observable diurnal effects on marine stratus albedo (and possibly droplet radius), further susceptibility calculations of an equivalent daily time-averaged albedo do not seem warranted. A detailed discussion of each topic in this section can be found in Platnick (1991).

## 4. Results

### a. Sensitivity

The retrievals and subsequent calculations of susceptibility generally depend on the cloud temperature and albedo, surface temperature (for thin clouds), atmospheric corrections in all channels, and calibrations used for AVHRR channels 1 and 2. A sensitivity study was made at three surface temperatures [±3 K about a nominal determined from the clear-sky SST algorithm of McClain et al. (1985)], two channel 1 surface albedos (0.06 and 0.03), three extreme atmospheric paths (corresponding to the nominal found from LOWTRAN for a path from the top of the boundary layer to the top of the atmosphere, one for a path from the surface to the top of the atmosphere, and one with no atmosphere at all), and two channel 1 calibrations (Che et al. 1991; Holben et al. 1991). Three adjacent cloud regions were studied from a *NOAA-11* HRPT image on 20 March 1989 in the vicinity of 30.5°N, 126°W; satellite viewing angles give resolutions of about 1.7 km. For susceptibility, the thin and moderately thick stratus regions ($\tau \approx 2$ and $\tau \approx 8$, respectively) show little sensitivity, usually less than a factor of 2. A thick cloud ($\tau \geq 25$) is highly variable in retrieved optical thickness as expected and susceptibility varies accordingly. For retrieved droplet size, the results suggest a rather robust solution for the moderately thick cloud where retrieved radii were within one library increment of each other (nominal was 8 μm) and optical thickness varied from 6 to 10 (nominal was 7.5). For all cloud regions, the radius never varied from the nominal solution by more than two library increments (one increment was typical). A detailed discussion of retrieval sensitivity is given in Platnick (1991).

### b. Comparison with some in situ measurements

A common difficulty in satellite remote sensing is comparison with in situ measurements. As a part of FIRE [First ISCCP (International Satellite Cloud Climatology Project) Regional Experiment], field observations were made of marine stratocumulus clouds off the coast of southern California in the summer of 1987. Two reports have been published of cloud microphysical measurements taken at times almost concurrent with the pass of a NOAA polar orbiter.

The aircraft measurements by Rawlins and Foot (1990) were taken over the course of several hours on the afternoon of 30 June 1987. Additional data from this flight was obtained from the Meteorological Research Flight of the U.K. Meteorological Office (J. P. Taylor 1991, personal communication). A run was made within and above a 300-m-thick cloud. Effective radii of about 9.0 μm were calculated from drop size distributions near cloud top. Optical thickness, estimated from their cloud reflectance data, varied from 15 to 60. We analyzed a *NOAA-9* AVHRR LAC (local area coverage) image, acquired within an hour of the in situ measurements, for a north–south flight path taken by the aircraft. In this region the solar and satellite zenith angles give $\mu_0 \approx 0.90$ and $\mu_{sat} \approx 0.50$, respectively (corresponding to a resolution of about 3.8 km). Because of the relatively large satellite viewing angle, atmospheric corrections were determined for this specific case. Figure 2 shows our retrievals, giving radii of 10 μm along the entire path with one pixel showing 8 μm; optical thickness varies from 20 to 70. Agreement

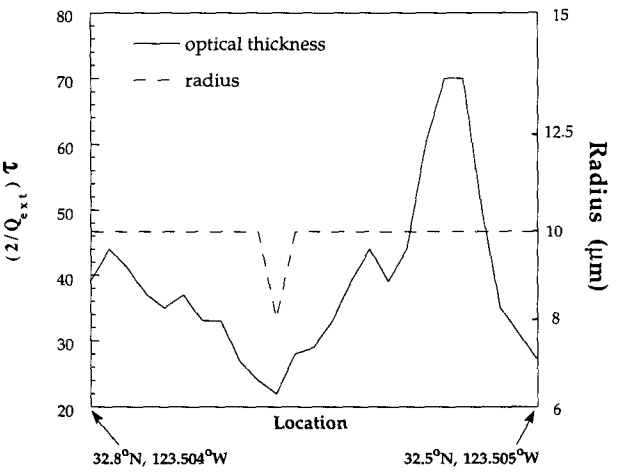


FIG. 2. Drop radius and optical thickness retrieved from a *NOAA-9* LAC image, 30 June 1987, along an aircraft flight track (about 100 km long) taken by Rawlins and Foot (1990) in stratocumulus off southern California.

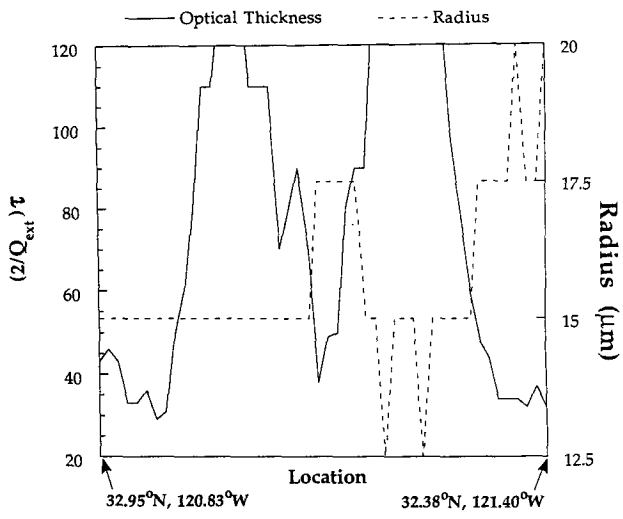


FIG. 3. Drop radius and optical thickness retrieved from a *NOAA-10* HRPT image, 10 July 1987, along a path crossing the ship tracks reported by Radke et al. (1989) in stratus off southern California.

between retrieved values of radius and the in situ measurements are within the radius increments available from the library data (at a radius of 10 $\mu$m, increments of +2.5, −2.0 $\mu$m in radius are possible to resolve with the library). Radius is not sensitive to the exact atmospheric correction applied. Susceptibility calculations made throughout the cloud region (not limited to the flight track), using Eq. (6) with a cloud liquid water content of 0.3 g $m^{-3}$, vary over an order of magnitude, from about $0.5 \times 10^{-3}$ (units of cubic centimeters will be assumed throughout this paper) at the northern end of the cloud to as high as $6.0 \times 10^{-3}$ at the southern end.

Radke et al. (1989) reported passage through two ship tracks within a stratocumulus cloud layer on 10 July 1987. Radiation and microphysical measurements were taken midway between the approximately 500-m-thick cloud. Droplet concentrations were seen to increase from 30 to 50 $cm^{-3}$ outside the track to over 100 $cm^{-3}$ within the track, indicative of larger CCN numbers. We obtained an HRPT *NOAA-10* image for this region ($\mu_0 \approx 0.50$, $\mu_{sat} \approx 0.79$ giving about 1.7-km resolution) that was captured 20 min before the measurements were made. We retrieved cloud parameters along two section lines crossing the tracks. The average retrieved radius, both in and out of the tracks, is typically 3–6 $\mu$m larger than the reported in situ measurements. Our retrievals for one of the section lines is shown in Fig. 3. Microphysical studies in California stratus typically show increasing droplet sizes with height (e.g., Noonkester 1984; Rawlins and Foot 1990). At the 3.75-$\mu$m wavelength, absorption is larger and therefore droplet sizes near cloud top contribute a greater influence to the inferred sizes than droplets farther down in the cloud where the in situ measurements were taken. Retrieved susceptibilities are, as expected, smaller in the ship tracks: $0.5 \times 10^{-3}$ in track and $1.0 \times 10^{-3}$–$2.0 \times 10^{-3}$ out of track. Susceptibilities calculated from the measured data are similar with $0.20 \times 10^{-3}$–$0.65 \times 10^{-3}$ in track and $0.70 \times 10^{-3}$–$1.45 \times 10^{-3}$ out of track.

Extensive wintertime fog in the central valleys of California is expected to contain large CCN concentrations from agricultural, industrial, and natural sources. This fog should be at the low end of the susceptibility scale, providing another check of the retrieval algorithm. Three *NOAA-11* GAC (global area coverage) images of valley fog from the winter of 1989/90 have been analyzed. Retrieved radius is especially uniform throughout the length of the valleys—typically 6–8 $\mu$m—smaller than for marine stratus as expected and in general agreement with the results of Garland (1971). Optical thickness ranged from 10 to over 100 (larger $\tau$ always found in the northern part of the Central Valley). Figure 4 shows an example of the retrievals for 20 December 1989. Susceptibility was as low as $0.05 \times 10^{-3}$, two orders of magnitude less than the larger values found in California marine stratus. This is probably a lower limit since liquid water content is likely to be less than the 0.3 g $m^{-3}$ used in the calculation.

### c. *California marine stratus and ship tracks*

Ship tracks may represent a microcosm for what is slowly occurring in the atmosphere. The direct applicability of ship track measurements to the prediction of global cloud albedo modification is not certain, however, and is discussed in the next section. For our purposes, stratus containing ship tracks is expected to have large variations in susceptibility over a small scale,

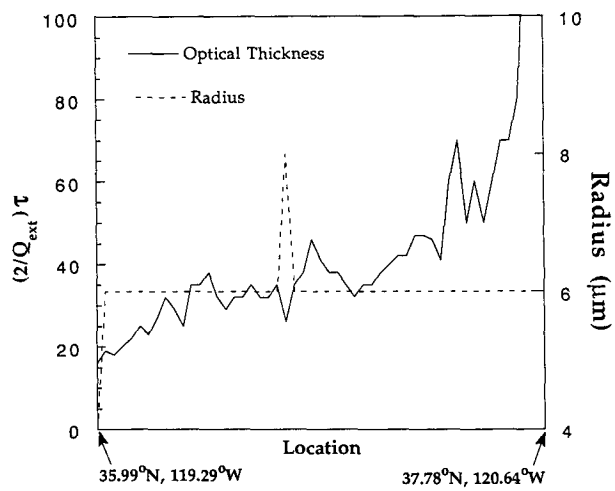


FIG. 4. Drop radius and optical thickness retrieved from a *NOAA-11* GAC image, 20 December 1989 along a path through California's Central Valley (about 200 km long) during extensive fog.

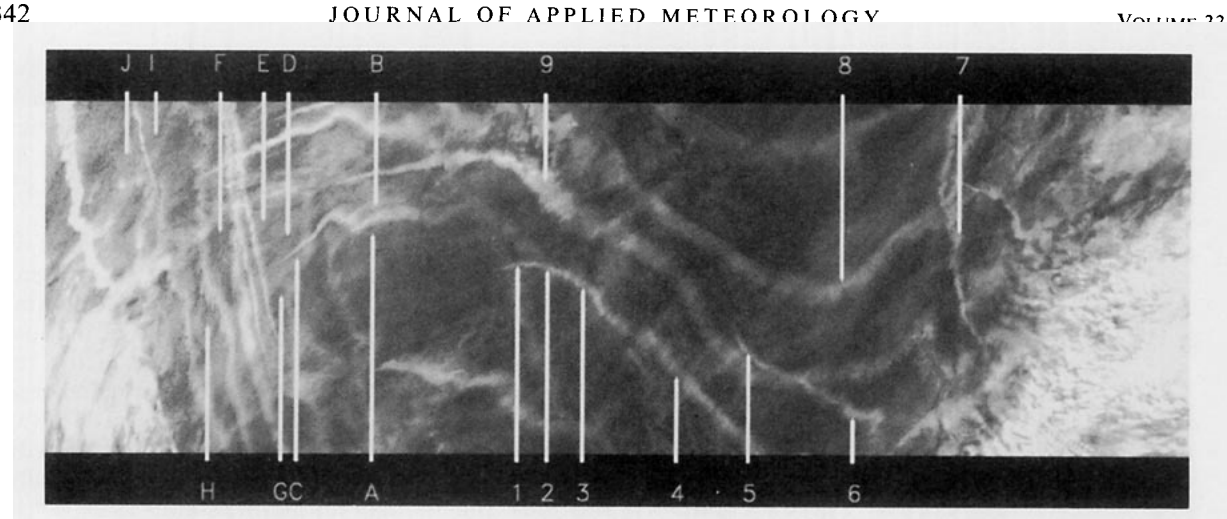


FIG. 5. AVHRR (*NOAA-11* HRPT) channel 1 image from 2 March 1990 of ship tracks in stratocumulus west of Washington State. Letters designate out-of-track locations where retrievals were made; number designations are for in-track locations. North is at the top of the image.

thus providing a useful test for sensing relative susceptibility; the solar and satellite viewing angles, cloud temperatures, surface properties, and atmospheric influences are similar, and so relative retrievals of cloud parameters are more credible than comparisons between distant regions. A dramatic instance of ship tracks is seen in an HRPT *NOAA-11* image from 2 March 1990 in a large region centered near 52°N, 140°W (see Fig. 5). Tracks are seen to be forming in uniform stratus to the west as well as in a thinner stratus region in the center of the image. Resolution is from 1 to 2 km. A number of locations in the image have been analyzed, including 13 individual tracks. Average results for out-of-track locations, designated by letters on the figure, are given in Table 1a; in-track results are given in Table 1b. Optical thickness and radius retrievals summarized in Fig. 6 clearly show smaller radii and larger optical thicknesses in the tracks. Three to five adjacent pixels were typically used to calculate the averages, designated by a single data point. Out-of-track retrievals are taken from the thicker western stratus only. A histogram of susceptibility is shown in Figure 7. Tracks in the thinner stratus give the smaller susceptibilities and smaller optical thicknesses; retrieved radii are about the same for both regions of tracks.

TABLE 1a. Retrieved results for selected out-of-track regions for *NOAA-11* HRPT, 2 March 1990. Each entry represents an average of 3–5 pixels.

| Location | Radius ($\mu$m) | Optical thickness | Susceptibility ($\times 10^{-3}$) | Liquid water path (g m$^{-2}$) |
|---|---|---|---|---|
| *A* | 15.6 | 4.9 | 3.42 | 51 |
| *B* | 14.7 | 8.1 | 2.87 | 79 |
| *C* | 15.6 | 5.7 | 3.42 | 59 |
| *D* | 17.2 | 6.0 | 4.61 | 69 |
| *E* | 14.2 | 6.4 | 2.60 | 61 |
| *F* | 18.3 | 4.0 | 5.62 | 49 |
| *G* | 19.2 | 4.0 | 6.74 | 51 |
| *H* | 15.0 | 5.8 | 3.30 | 59 |
| *I* | 19.4 | 6.7 | 6.63 | 87 |
| *J* | 18.9 | 7.3 | 6.10 | 92 |

### d. *Some observations on ship tracks*

Though the emphasis of this study is on susceptibility, the results for the 2 March 1990 image allow for a few comments regarding ship tracks themselves. There is some suggestion of horizontal entrainment of the track into nearby regions. The first two tracks be-

TABLE 1b. Retrieved results for selected in-track regions for *NOAA-11* HRPT, 2 March 1990. Each entry represents an average of 3–5 pixels. Multiple tracks found between letter-designated locations are given in order from east to west.

| Location | Radius ($\mu$m) | Optical thickness | Susceptibility ($\times 10^{-3}$) | Liquid water path (g m$^{-2}$) |
|---|---|---|---|---|
| *A–B* | 12.5 | 10.8 | 1.72 | 90 |
| *C–D* | 10.0 | 10.0 | 0.89 | 67 |
| *E–F* | 13.0 | 13.6 | 2.02 | 118 |
| | 12.5 | 18.3 | 1.59 | 153 |
| *G–H* | 10.0 | 10.0 | 0.98 | 67 |
| | 10.0 | 17.0 | 0.91 | 113 |
| | 13.2 | 15.9 | 2.21 | 140 |
| | 12.5 | 15.2 | 1.83 | 127 |
| *I–J* | 11.0 | 13.0 | 1.43 | 95 |
| 1 | 8.0 | 9.5 | 0.46 | 51 |
| 2 | 8.0 | 7.3 | 0.46 | 39 |
| 3 | 8.0 | 6.4 | 0.46 | 34 |
| 4 | 10.0 | 6.0 | 0.90 | 40 |
| 5 | 10.0 | 7.8 | 0.90 | 52 |
| 6 | 10.0 | 8.5 | 0.89 | 57 |
| 7 | 12.5 | 8.3 | 1.75 | 69 |
| 8 | 10.0 | 11.3 | 0.88 | 75 |
| 9 | 12.5 | 10.1 | 1.73 | 84 |

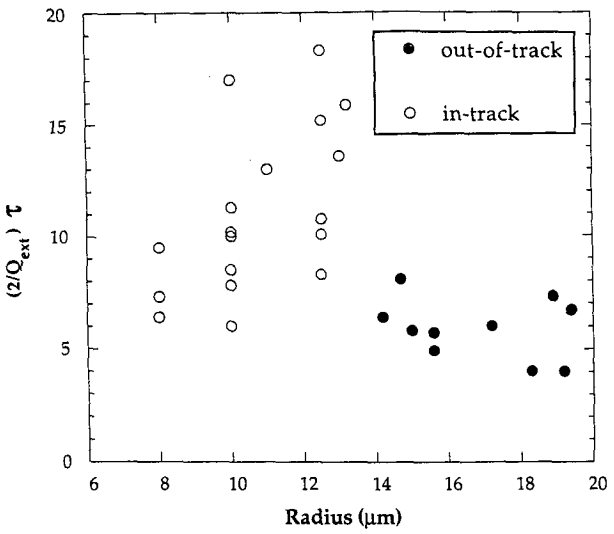


FIG. 6. Scattergram of retrieved radius and optical thickness in a stratocumulus cloud containing ship tracks (see Fig. 5); from *NOAA-11* HRPT, 2 March 1992.

tween locations *G* and *H* (going from east to west) appear to be younger tracks than the last two and have smaller radii (10 versus 13 μm) and susceptibilities (by a factor of 2). For locations 1, 2, and 3, optical thickness decreased slightly (9.5 to 6.4) when moving away from the head of the track. In some cases, however, no significant or systematic change in the retrieved values can be noted along the length of a track. No difference is seen between locations 5 and 6 (each with $r = 10$ μm, $\tau = 8$), though further analysis showed retrieved radius and optical thickness of 8 μm and 3, respectively, at the head of the track. The track referenced by location 7 showed a radius of 6.0 μm farther to the south, then increasing again to 10.0 μm closer to the head of the track; optical thickness increased to 14 and then decreased to 7. A general conclusion, but not a rule, is that the more diffuse or widespread the track, the larger the radii and the susceptibility (however, the narrow track between locations *I* and *J* has a relatively large radius and susceptibility compared with other narrow tracks). There appears to be some limit to the horizontal spreading of the tracks, at least over relatively short periods of time. For example, the tracks running from north to south between locations *G* and *H* show little spread over a distance of about 100 km and the track between locations *I* and *J* is similar. Radke et al. (1989) state that ship tracks are not brighter at their head and suggest that gases responsible for CCN production horizontally diffuse before particles develop. The results for locations 1–4, mentioned above, argue against the generality of this notion. For that track, optical thickness increased (i.e., brighter track) toward the head of the track though radius remained constant. This was not necessarily true for other tracks, however. It may also be that CCN (not the precursor gases) can diffuse before cloud nucleation occurs; the mechanisms for cloud nucleation are not clear and should not be presumed to be uniform spatially or temporally. Still, the fine point seen at the head of many tracks, and the results from locations 1–4, indicates that nucleation often occurs before CCN, or gases responsible for CCN production, are allowed to diffuse substantially.

Radke et al. (1989) measured increases in liquid water content in ship tracks compared with the surrounding cloud. Liquid water paths given in Table 1 show similar results for the western stratus (indicated with letter designations), assuming constant cloud geometrical thickness in and out of the track. Based on results from Albrecht (1989), Radke et al. proposed that the smaller droplet sizes in ship tracks suppressed the formation of drizzle drops, resulting in the higher liquid water contents. It might also be possible that some aspect of the ship (e.g., a warm plume, wake effects, etc.) locally modifies the boundary layer and enhances cloud formation. When tracks form in mature stratus, supersaturations would normally be too low to activate new CCN. Either cloud dynamics or some ship-induced mechanism must allow for the scavenging of existing liquid water for new droplet growth. The tracks seen in the center of the image have similar radii and optical thicknesses to those in the thicker stratus to the west but yet have formed in a region that was evidently not as conducive to substantial stratus development. If the ship itself is partially responsible for allowing activation of new CCN, other aspects of the track, such as its liquid water content, may also be modified. If so, implicating the observable increase in liquid water content with the suppression of drizzle may not always be valid. With the special circumstances involved in ship track development, it is not at all clear that the global susceptibility of marine

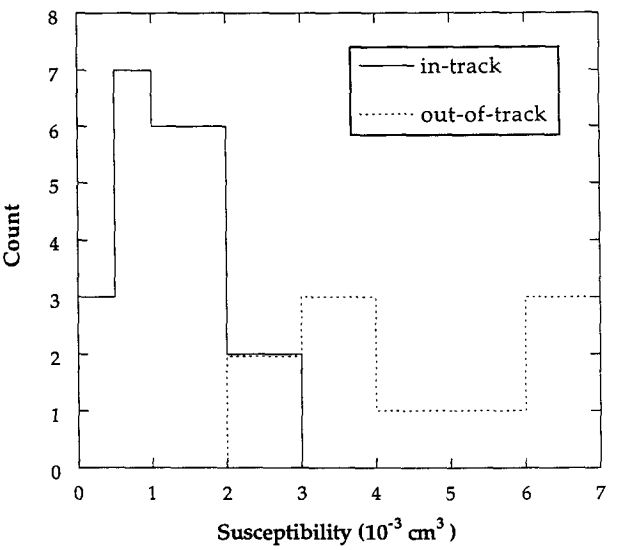


FIG. 7. Histogram of cloud susceptibilities for the retrievals of Fig. 6.

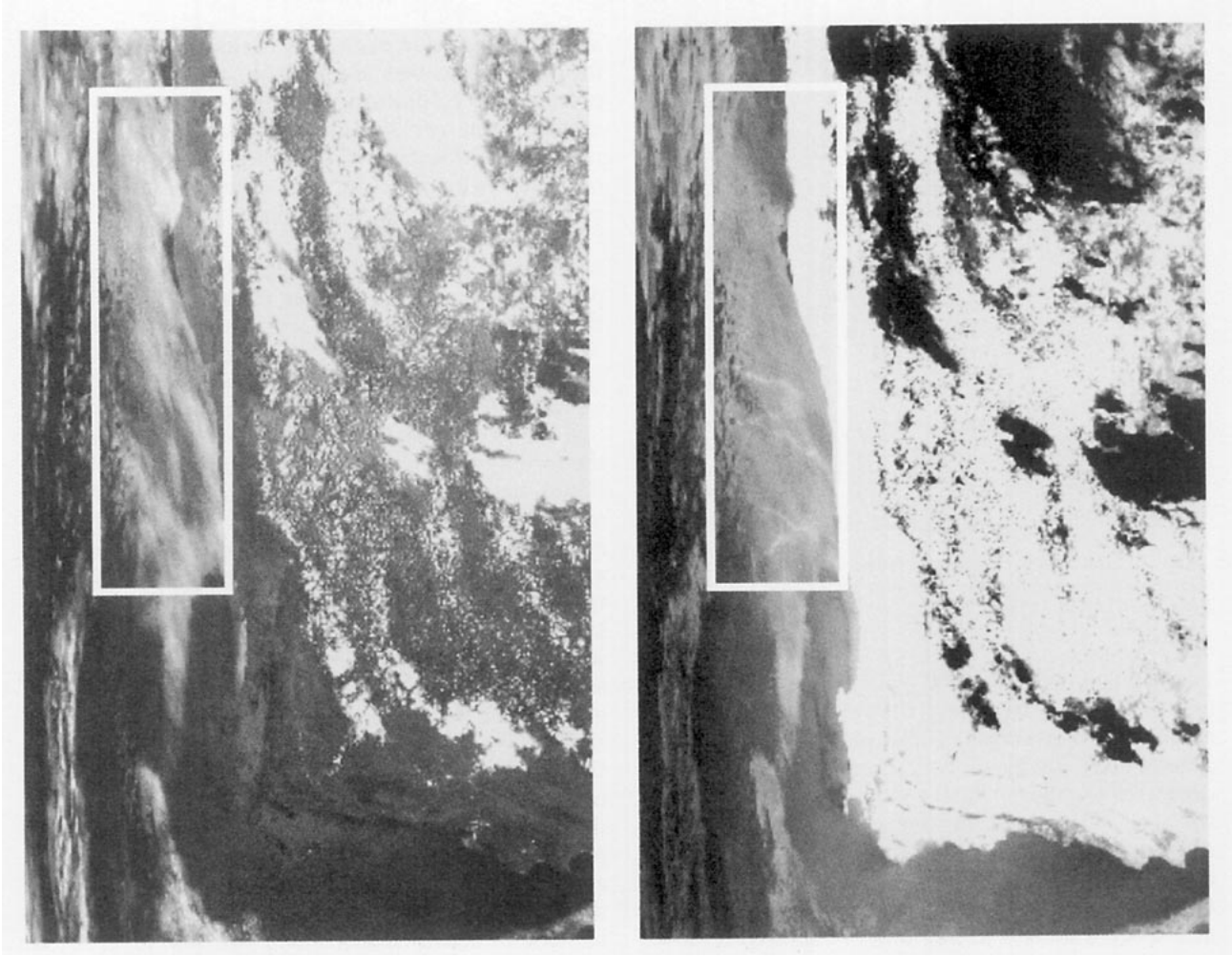

FIG. 8. AVHRR *NOAA-11* GAC channels 1 (left) and 3 (right) image from 4 January 1989 of stratus off the coast of Namibia. North is at the top of the image.

stratus would be equally affected by this drizzle suppression. However, if proved true, this would serve to increase susceptibilities as shown in Eq. (9). The difference in radii between in-track and out-of-track cloud regions ranged from about 2 to 10 $\mu$m. Assuming the power-law relation used in deriving Eq. (9), the following relation would exist between changes in radius and cloud droplet concentration: $\Delta N/N = (1 + \Delta r/r) \exp[-3/(1-\beta)] - 1$. So, typically retrieved changes in radius from $\Delta r/r = -0.15$ to $-0.3$ give corresponding changes in droplet concentration of about $\Delta N/N = 1$ to 5, respectively, with no change in liquid water content ($\beta = 0$) $\Delta N/N = 0.6$ to 1.9, respectively.

Several other images of California stratus were analyzed, some showing ship tracks. In general, susceptibility alone was not a sufficient predictor of tracks. Relatively high susceptibilities were often found in clouds not containing tracks. Though ship tracks are common, they are absent more often than not despite the likely constant presence of ship traffic. It is reasonable to assume that cloud dynamics plays an important role in the nucleation of ship-produced CCN and must be considered along with the microphysics.

### *e. Marine stratus near southern Africa*

Marine stratus is quite common, especially near the western coasts of the continents. Two *NOAA-11* GAC images in the South Atlantic, off the coast of Namibia and South Africa (4 January 1989 and 19 April 1989 with resolution of 5–6 km), were analyzed. The stratus from both days is located near the coast and is extensive and isolated. The image for 4 January 1989 is shown in Fig. 8; analysis is limited to stratus within the box. Retrievals gave 6.0- to 9.0-$\mu$m radii, optical thicknesses from 3 to 12, and susceptibilities from $0.2 \times 10^{-3}$ to $0.8 \times 10^{-3}$. Analysis of the linear cloud features appearing in the channel 3 image does not suggest that they are ship tracks. It is impossible to make any climatological conclusion regarding the microphysics of this stratus, but for the two cases studied, radii and susceptibilities are much less than those typically found

in uncontaminated California stratus. Either larger CCN concentrations are found here, or the liquid water content of the clouds is much smaller (by a fraction of about 0.15–0.30). The small radii and susceptibilities are unexpected for this presumably clean region. If these results were generally true, it might explain the lack of ship track sightings in this region even though stratus development is common.

A *NOAA-11* GAC from 22 January 1989 was analyzed for a region south of Madagascar in the Indian Ocean (33.3°S, 45.71°E, see Fig. 9). Satellite viewing angles are near nadir giving 4-km resolution. Two likely ship tracks are seen forming in a broken stratocumulus deck. There is an obvious reduction in droplet size in the apparent tracks (8 $\mu$m versus 12.5–17.5 $\mu$m for out-of-track regions) and larger optical thicknesses (8–15 versus 3–12 out of track). The broken clouds seen in the image can give misleading results if analyzed pixels are not completely cloud filled. However, care was taken to analyze only neighboring pixels having the largest optical thicknesses for a particular area. With this caveat, calculated susceptibilities are consistent with the expectations for ship tracks and are comparable to those found in California stratus. (To the authors' knowledge, this would be the first report of ship tracks being found in the Southern Hemisphere.)

## 5. Summary

A definition of cloud susceptibility has been proposed as a measure of the extent of CCN influence on cloud albedo. Its calculation, requiring inference of optical thickness and microphysics, was originally couched in terms of $\tau \partial A/\partial \tau$ and cloud droplet concentration $N$. However, $N$ cannot be found directly from cloud reflection measurements but must be inferred from the droplet radius, which can be sensed, and an assumption regarding the value of cloud liquid water content. Susceptibilities were normalized to a liquid water content of 0.3 g $m^{-3}$, a representative value for marine stratus. Analysis of several AVHRR images has been presented. Retrieved radius and optical thick-

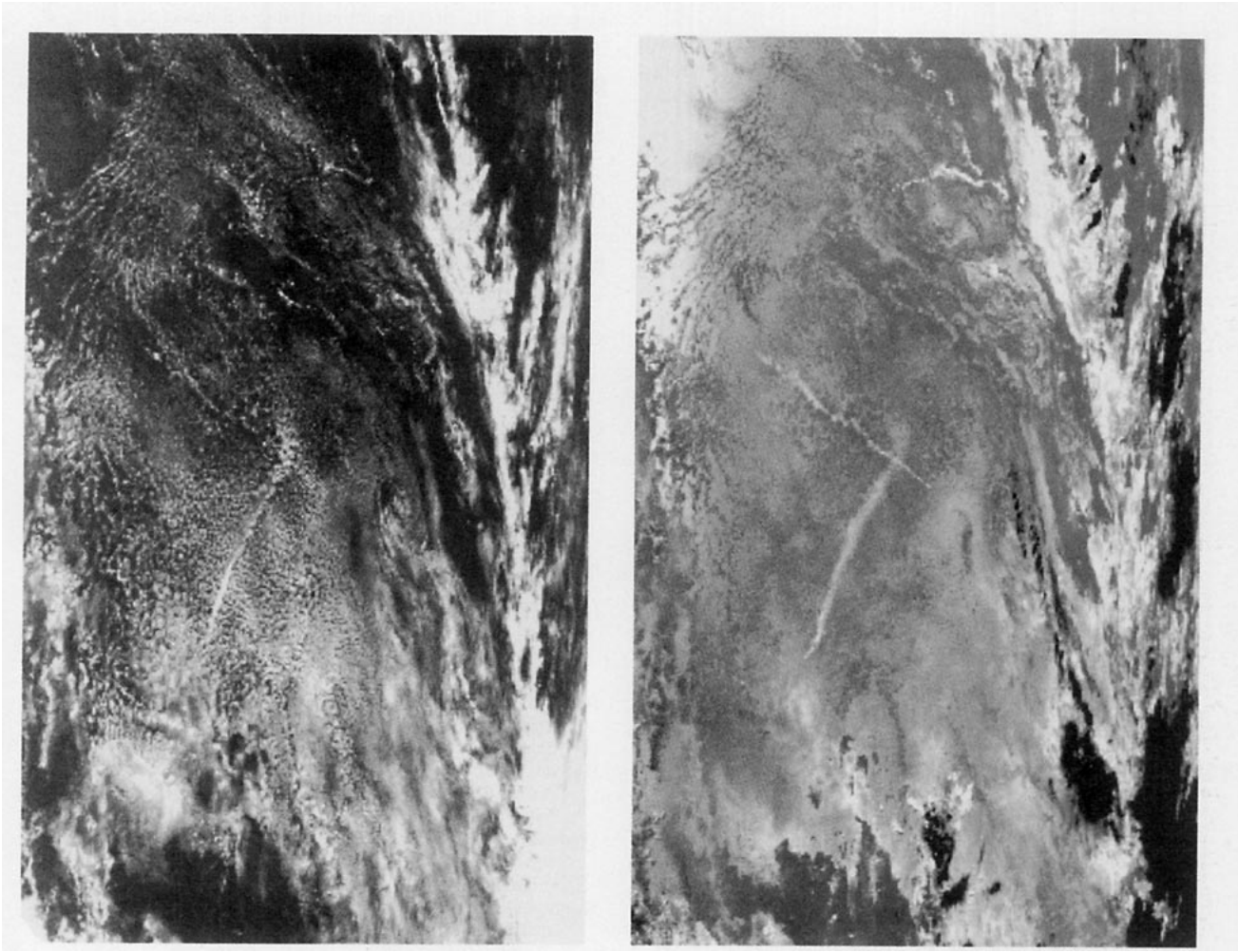

FIG. 9. AVHRR *NOAA-11* GAC channels 1 (left) and 3 (right) image from 22 January 1989 of stratocumulus south of Madagascar. North is at the top of the image.

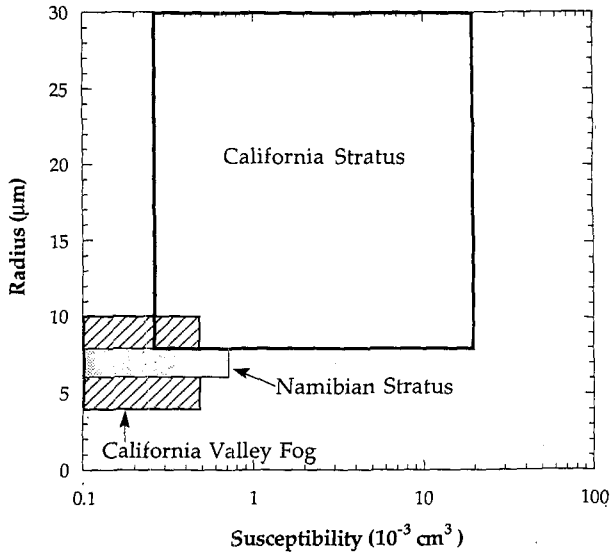


FIG. 10. A schematic summary for the range of drop radius and cloud susceptibility retrieved during this study.

ness using the method of this study compared well with in situ measurements made by two groups of investigators during FIRE in 1987. California valley fog provided a test for small susceptibilities.

The retrieved range of susceptibilities (in units of cubic centimeters) for the marine clouds studied varied by about two orders of magnitude; from as low as $0.23 \times 10^{-3}$ in stratus off the west coast of southern Africa to about $20 \times 10^{-3}$ in thin stratus off the California coast. This range implies that studies of marine stratus albedo modification from anthropogenic CCN must account for existing variations in susceptibility. Susceptibilities for California valley fog were as low as $0.05 \times 10^{-3}$, extending the measured range for all clouds studied to almost three orders of magnitude. Figure 10 shows a schematic representation for the range of retrieved radii and susceptibilities found in this study. However, the largest radii and susceptibilities retrieved in the California stratus correspond to clouds with small optical thicknesses where surface effects (reflection and emission) are important. Studies in ship tracks have shown that the tracks are indeed less susceptible than out-of-track regions. The susceptibility differs by a factor of 2–4 up to as high as 30 for thin stratus. The use of susceptibility extends beyond fog and marine stratus, which have been highlighted in this study because of their relative homogeneity for remote sensing purposes.

*Acknowledgments.* One of the authors (S.P.) would like to thank F. P. J. Valero and P. Pilewskie of NASA/Ames Research Center for their encouragement and support during the writing of this paper, and the National Research Council research associate program. This work was supported by NSF Grant ATM-8716637 through the Institute of Atmospheric Physics, University of Arizona, Tucson.

## REFERENCES

Albrecht, B. A., 1989: Aerosols, cloud microphysics, and fractional cloudiness. *Science,* **245,** 1227–1230.

Arking, A., 1991: The radiative effects of clouds and their impact on climate. *Bull. Amer. Meteor. Soc.,* **71,** 795–813.

——, and K. Grossman, 1972: The influence of line shape and band structure on temperatures in planetary atmospheres. *J. Atmos. Sci.,* **29,** 937–949.

——, and J. D. Childs, 1985: Retrieval of cloud cover parameters from multispectral satellite images. *J. Climate Appl. Meteor.,* **24,** 322–333.

Bohren, C. F., 1980: Multiple scattering of light and some of its observable consequences. *Amer. J. Phys.,* **55,** 524–533.

Charlson, R. J., J. E. Lovelock, M. O. Andreae, and S. G. Warren, 1987: Oceanic phytoplankton, atmospheric sulphur, cloud albedo and climate. *Nature,* **326,** 655–661.

——, S. E. Schwartz, J. M. Hales, R. D. Cess, J. A. Coakley, Jr., J. E. Hansen, and D. J. Hofmann, 1992: Climate forcing by anthropogenic aerosols. *Science,* **255,** 423–430.

Che, N., B. G. Grant, D. E. Flittner, P. N. Slater, S. F. Biggar, 1991: Results of Calibrations of the NOAA-11 AVHRR made by reference to calibrated SPOT imagery at White Sands, N.M. *Proc. SPIE,* **1493.**

Dinger, J., H. B. Howell, and T. H. Wojciechowski, 1970: On the source and composition of cloud nuclei in a subsident air mass over the North Atlantic. *J. Atmos. Sci.,* **27,** 791–797.

Feigelson, E. M., 1978: Preliminary radiation model of a cloudy atmosphere. 1. Structure of clouds and solar radiation. *Beitr. Phys. Atmos.,* **51,** 203–229.

Foot, J. S., 1988: Some observations of the optical properties of clouds. I: Stratocumulus. *Quart. J. Roy. Meteor. Soc.,* **114,** 129–144.

Fouquart, Y., J. C. Buriez, M. Herman, and R. S. Kandel, 1990: The influence of clouds on radiation: A climate-modeling perspective. *Rev. Geophys.,* **28,** 145–166.

Garland, J. A., 1971: Some fog droplet size distributions obtained by an impaction method. *Quart. J. Roy. Meteor. Soc.,* **97,** 483–494.

Ghan, S. J., K. E. Taylor, J. E. Penner, and D. J. Erickson, III, 1990: Model test of CCN–cloud albedo climate forcing. *Geophys. Res. Lett.,* **17,** 607–610.

Gorbinet, G., and R. Serpoly, 1985: Influence of an industrial site on the characteristics of CCN supersaturation spectra associated with air masses of different origin. *J. Rech. Atmos.,* **19,** 193–202.

Grainger, R. G., 1990: The calculation of cloud parameters from AVHRR data. Ph.D. dissertation, University of Auckland, New Zealand, 188 pp.

Grassl, H., 1982: The influence of aerosol particles on radiation parameters of clouds. *Időjárás, J. Hungarian Meteor. Soc.,* **86,** 60–75.

Hansen, J. E., and L. D. Travis, 1974: Light scattering in planetary atmospheres. *Space Sci. Rev.,* **16,** 527–610.

Hegg, D. A., L. F. Radke, and P. V. Hobbs, 1991: Measurements of Aitken nuclei and cloud condensation nuclei in the marine atmosphere and their relation to the DMS-cloud-climate hypothesis. *J. Geophys. Res.,* **96,** 18 727–18 733.

Hobbs, P. V., J. L. Stith, and L. F. Radke, 1980: Cloud-active nuclei from coal-fired electric power plants and their interaction with clouds. *J. Appl. Meteor.,* **19,** 439–451.

Holben, B. N., Y. J. Kaufman, and J. D. Kendall, 1990: NOAA-11 AVHRR visible and near-IR inflight calibration. *Int. J. Remote Sens.,* **11,** 1511–1519.

Hudson, J. G., and C. F. Rogers, 1986: Relationship between critical supersaturation and cloud droplet size: Implications for cloud mixing processes. *J. Atmos. Sci.,* **43,** 2341–2359.

Kaufman, Y. J., R. S. Fraser, and R. L. Mahoney, 1991: Fossil fuel and biomass burning effect on climate—Heating or cooling? *J. Climate,* **4,** 578–588.

Kneizys, F. X., E. P. Shettle, L. W. Abrev, J. H. Chetwynd, G. P. Anderson, W. O. Gallery, J. E. A. Selby, and S. A. Clough,

1988: User's guide to LOWTRAN 7. AFGL-TR-88-0177, Air Force Geophysics Laboratory, Hanscom Air Force Base, MA, 146 pp.

Laszlo, I., H. Jacobowitz, and A. Gruber, 1988: The relative merits of narrowband channels for estimating broadband albedo. *J. Atmos. Oceanic Technol.*, **5,** 757–773.

Leaitch, W. R., G. A. Isaac, J. W. Strapp, C. M. Banic, and H. A. Wiebe, 1992: The relationship between cloud droplet number concentrations and anthropogenic pollution: Observations and climatic implications. *J. Geophys. Res.*, **97,** 2463–2474.

Martin, G. M., and D. W. Johnson, 1992: The measurements and parameterizations of effective radius of droplets in stratocumulus clouds. *Int. Commission on Clouds and Precipitation, Proc.* Montreal.

McClain, E. P., W. G. Pichel, and C. C. Walton, 1985: Comparative performance of AVHRR-based multichannel sea surface temperatures. *J. Geophys. Res.*, **90,** 11587–11601.

Neckel, H., and D. Labs, 1984: Solar radiation between 3000 and 12500 Å. *Sol. Phys.*, **90,** 205–258.

Noonkester, V. R., 1984: Droplet spectra observed in marine stratus cloud layers. *J. Atmos. Sci.*, **41,** 829–845.

Penner, J. E., R. E. Dickinson, and C. A. O'Neill, 1992: Effects of aerosol from biomass burning on the global radiation budget. *Science,* **256,** 1432–1433.

Platnick, S., 1991: Remote sensing the susceptibility of cloud albedo to changes in drop concentration. Ph.D. dissertation, University of Arizona.

Radke, L. F., J. A. Coakley, and M. D. King, 1989: Direct and remote sensing observations of the effects of ships on clouds. *Science,* **246,** 1146–1149.

Rawlins, F., and J. S. Foot, 1990: Remotely sensed measurements of stratocumulus properties during FIRE using the C130 aircraft multi-channel radiometer. *J. Atmos. Sci.*, **47,** 2488–2503.

Shine, K. P., A. Henderson-Sellers, and A. Slingo, 1984: The influence of the spectral response of satellite sensors on estimates of broadband albedo. *Quart. J. Roy. Meteor. Soc.*, **110,** 1170–1179.

Slingo, A., S. Nicholls, and J. Schmetz, 1982: Aircraft observations of marine stratocumulus during JASIN. *Quart. J. Roy. Meteor. Soc.*, 833–856.

Somerville, R. C. J., and L. A. Remer, 1984: Cloud optical thickness feedbacks in the $CO_2$ climate problem. *J. Geophys. Res.*, **89,** 9668–9672.

Squires, P., 1966: An estimate of the anthropogenic production of cloud nuclei. *J. Rech. Atmos.*, **2,** 297–308.

Stephens, G. L., and C. M. R. Platt, 1987: Aircraft observations of the radiative and microphysical properties of stratocumulus and cumulus cloud fields. *J. Climate Appl. Meteor.*, **26,** 1243–1269.

——, and S. Tsay, 1990: On the cloud absorption anomaly. *Quart. J. Roy. Meteor. Soc.*, **116,** 671–704.

Taylor, J. P., 1992: Sensitivity of remotely sensed effective radius of cloud droplets to changes in LOWTRAN version. *J. Atmos. Sci.*, **49,** 2564–2569.

Teillet, P. M., P. N. Slater, Y. Ding, R. P. Santer, R. D. Jackson, and M. S. Moran, 1990: Three methods for the absolute calibration of the NOAA AVHRR sensors in-flight. *Remote Sens. Environ.*, **31,** 105–120.

Twomey, S., 1959: The nuclei of natural cloud formation. *Geofis. Pura. Appl.*, **43,** 243–249.

——, 1968: On the composition of cloud nuclei in the northeastern United States. *J. Rech. Atmos.*, **3,** 281–285.

——, 1974: Pollution and the planetary albedo. *Atmos. Environ.*, **8,** 1251–1256.

——, 1977: The influence of pollution on the shortwave albedo of clouds. *J. Atmos. Sci.*, **34,** 1149–1152.

——, 1991: Aerosols, clouds amd radiation. *Atmos. Environ.*, **254,** 2435–2442.

——, and J. Warner, 1967: Comparison of measurements of cloud droplets and cloud nuclei. *J. Atmos. Sci.*, **24,** 702–703.

——, and T. A. Wojciechowski, 1969: Observations of the geographical variation of cloud nuclei. *J. Atmos. Sci.*, **26,** 684–688.

——, and T. Cocks, 1982: Spectral reflectance of clouds in the near-infrared: comparison of measurements and calculations. *J. Meteor. Soc. Japan,* **60,** 583–592.

——, and ——, 1989: Remote sensing of cloud parameters from spectral reflectance measurements in the near-infrared. *Beitr. Phys. Atmos.*, **62,** 172–179.

——, H. Jacobowitz, and H. B. Howell, 1966: Matrix methods for multiple scattering problems. *J. Atmos. Sci.*, **23,** 101–108.

Warner, J., and S. Twomey, 1967: The production of cloud nuclei by cane fires and the effect on cloud droplet concentration. *J. Atmos. Sci.*, **24,** 704–706.

Wydick, J., A. Davis, and A. Gruber, 1987: Estimation of broadband planetary albedo from operational narrowband satellite measurements. NOAA Tech. Rep. NESDIS 27.